Systems/Circuits

Medial Prefrontal Cortex Inversely Regulates Toluene-Induced Changes in Markers of Synaptic Plasticity of Mesolimbic Dopamine Neurons

Jacob T. Beckley, Caitlin E. Evins, Hleb Fedarovich, Meghin J. Gilstrap, and John J. Woodward

Department of Neurosciences, and Center for Drug and Alcohol Programs, Department of Psychiatry, Medical University of South Carolina, Charleston, South Carolina 29425

Toluene is a volatile solvent that is intentionally inhaled by children, adolescents, and adults for its intoxicating effects. Although voluntary use of toluene suggests that it possesses rewarding properties and abuse potential, it is unknown whether toluene alters excitatory synaptic transmission in reward-sensitive dopamine neurons like other drugs of abuse. Here, using a combination of retrograde labeling and slice electrophysiology, we show that a brief *in vivo* exposure of rats to a behaviorally relevant concentration of toluene vapor enhances glutamatergic synaptic strength of dopamine (DA) neurons projecting to nucleus accumbens core and medial shell neurons. This effect persisted for up to 3 d in mesoaccumbens core DA neurons and for at least 21 d in those projecting to the medial shell. In contrast, toluene vapor exposure had no effect on synaptic strength of DA neurons that project to the medial prefrontal cortex (mPFC). Furthermore, infusion of GABAergic modulators into the mPFC before vapor exposure to pharmacologically manipulate output, inhibited, or potentiated toluene's action on mesoaccumbens DA neurons. Together, the results of these studies indicate that toluene induces a target-selective increase in mesolimbic DA neuron synaptic transmission and strongly implicates the mPFC as an important regulator of drug-induced plasticity of mesolimbic dopamine neurons.

Introduction

A single exposure to behaviorally active doses of drugs of abuse, such as cocaine, ethanol, nicotine, and benzodiazepines, has been shown to induce marked alterations in glutamatergic synapses on dopamine (DA) neurons in the ventral tegmental area (VTA) (Mansvelder and McGehee, 2000; Ungless et al., 2001; Saal et al., 2003; Heikkinen et al., 2009). These changes, which can persist for prolonged periods of time, are thought to reflect the initiation of altered glutamatergic signaling in an addiction neurocircuitry that underlies the development of drug dependence. This notion is supported by anatomical studies demonstrating that midbrain DA neurons and ventral and dorsal striatum are interconnected in a cascade of reciprocal loops (Haber et al., 2000; Everitt and Robbins, 2005). Results from other experiments have shown that persistent alterations in synaptic processes of VTA and nucleus accumbens (NAc) neurons after drug exposure are affected hierarchically, with VTA alterations being necessary for downstream synaptic changes in NAc medium spiny neurons (Mameli et al.,

2009). Alterations in excitatory synaptic transmission in VTA dopamine neurons are thus considered a signature event that predicts whether a given drug has abuse potential (Lüscher and Malenka, 2011).

Abused inhalants, such as the volatile solvent toluene, are an understudied class of drugs that have abuse liability and high rates of use among children and adolescents (Lubman et al., 2008). Like other abused drugs, toluene produces conditioned place preference in rodents, a behavioral indicator of positive reinforcement (Lee et al., 2006). Toluene also increases dopamine release in the NAc by enhancing the rate of VTA DA neuron firing (Riegel et al., 2007). Although there is evidence to suggest that toluene alters the addiction neurocircuitry similar to that of other drugs of abuse, it is not known whether abused inhalants, administered *in vivo*, significantly modify synaptic transmission on reward-responsive VTA DA neurons.

The study of drug-induced enduring changes in VTA DA neurons is complicated by findings from recent studies showing that VTA DA neurons exhibit biochemical and physiological diversity (Ford et al., 2006; Bjorklund and Dunnett, 2007; Lammel et al., 2008) and that drugs, such as cocaine, alter excitatory synaptic strength only in discrete subpopulations of DA neurons (Lammel et al., 2011). Therefore, in this study, we examined the effects of a single, brief *in vivo* exposure of rats to toluene vapor on physiological markers of synaptic plasticity in discrete VTA DA neuron subpopulations. Using a fluorescent retrograde tracer injected into axonal target areas, we selectively recorded from VTA DA neurons that projected to the NAc core (NAcc), NAc medial shell (NAcs), or medial prefrontal cortex (mPFC). In this way, we

A

Surgery   Pre-Exposure   Exposure

10-15d   Day 1   Day 2

5 | 10 | 10 | 10 | 25

60m air control

B

5000 PPM Toluene

H
T
X

t (min)

C

8% Toluene
4% Toluene

[Toluene] (PPM)

D

8% Toluene

t (min)

Figure 1. Analysis of toluene vapor concentration by gas chromatography. **A**, Schematic of experimental design. Toluene exposures are marked by the gray boxes. **B**, Sample chromatogram from 5000 PPM. H, Hexane; T, toluene; X, o-xylene. **C**, Standard curve showing the ratio of toluene and o-xylene area under the curve ($r^2 = 0.991$; $n = 5$ for each). Open circles represent the measured concentrations from 4 and 8% toluene exposures in the vapor chamber ($n = 5$ for each). **D**, Representative chromatogram from an air sample from the vapor chamber when 8% toluene is flowing at a rate of 4 L/min for 10 min.

aimed to determine whether toluene exposure results in altered excitatory synaptic transmission within different VTA DA neuron subpopulations.

Materials and Methods

Subjects. Male Sprague Dawley rats (Harlan) were housed in polypropylene cages with *ad libitum* access to food and water. Subjects were maintained in a climate-controlled room on a reverse light-dark cycle (lights off at 0900 h). All procedures were performed according to Medical University of South Carolina Institutional Animal Care and Use Committee protocols.

Stereotaxic surgery. Rats (postnatal day 24–34) underwent stereotaxic surgery under isoflurane anesthesia. A 150- to 250-nl volume of Retrobeads (Lumafluor) was injected into either the NAcc (rostral: +2.0 mm, lateral: ±1.4 mm, ventral: −6.0 mm), NAcs (rostral: +2.0 mm, lateral ±0.8 mm, ventral: −6.2 mm), or mPFC (rostral: +2.8 mm, lateral ±0.5 mm, ventral: −3.0 mm). In some experiments, after retrobead injection, rats were implanted with a 26-gauge bilateral guide cannula (intercannula width 1 mm; PlasticsOne) into the mPFC (rostral to bregma: +2.8 mm, lateral: ±0.5 mm, ventral −2.0 mm). Because the subjects underwent surgery during adolescence, we began with measurements using coordinates from an atlas of adult rats (Paxinos and Watson, 2005) and then made adjustments for more accurate injections and cannula implantations.

mPFC microinjection. A bilateral 33-gauge injection cannula (PlasticsOne) that extended 1 mm below the guide cannula was connected to PE20 tubing and attached to a 10-μl Hamilton syringe. Subjects were injected with 0.5 μl 0.9% sterile saline vehicle, 100 ng picrotoxin (Tocris Bioscience), or 130 ng baclofen (Abcam Biochemicals)/3.5 ng muscimol (Abcam Biochemicals) using a syringe pump (Harvard Apparatus) at a flow rate of 0.25 μl/min. Microinjections occurred 30 min before vapor chamber exposure.

Toluene vapor treatment. On day 1 (d1), subjects (P40-P47 d) were habituated to the vapor chamber (30 × 30 × 30 cm) for 30 min with continuous airflow at 4 L/min. On the following day, subjects were placed in the vapor chamber for 5 min and then toluene vapor was introduced into the chamber using a sevoflurane vaporizer. A setting of 4% resulted in a calculated vapor concentration of 2850 PPM toluene, and the 8% setting yielded 5700 PPM toluene. Vapor concentrations inside the chamber were confirmed using gas chromatography (Materials and Methods: Gas chromatography). The toluene concentrations

used in this study are well within the range used by human solvent abusers (Lubman et al., 2008) and have been used in previous animal studies (Gerasimov et al., 2002; Koga et al., 2007). Toluene-exposed subjects received two 10-min exposures of 5700 PPM or 2850 PPM toluene with an intertrial interval of 10 min. The airflow was maintained at 4 L/min at all times. Our toluene exposure paradigm was modeled after the common approach that inhalant abusers use to get intoxicated and involves several bouts of high concentration, short duration exposures to solvent vapor (Lubman et al., 2008). After the second exposure, rats stayed in the chamber for an additional 25 min. Air control animals stayed in the chamber for a total of 60 min, the same duration as toluene-exposed animals. Figure 1A contains a schematic that summarizes the vapor chamber exposure paradigm.

Gas chromatography. A Shimadzu GC-2010 gas chromatograph with flame ionization detector and an HP-FFAP column (ID, 0.53 mm; length, 30 m; film thickness, 1 μm; Agilent Technologies) was used to measure toluene samples. A fixed concentration of ortho-xylene (~7700 PPM) was used in all samples as an internal standard, and hexane was used to clean the gas-tight injector syringe and to dilute toluene standards. Because hexane was only combined with toluene to make known toluene standard concentrations, hexane peaks were large in standard samples but negligible in samples taken from the vapor chamber (Fig. 1B–D). Toluene vapor samples were measured with the following settings: manual injection, 500 μl; injector port temperature, 230°C; split ratio injection, 10:1; column flow rate, 3 ml/min (carrier gas: helium); program, 60°C for 5 min; flame ionization detector temperature, 230°C; helium gas flow, 30 ml/min; hydrogen gas flow, 40 ml/min; air flow, 400 ml/min. Peaks were clearly discriminated and located at (in minutes): hexane 0.52, toluene 1.52, o-xylene 3.29.

Standard solutions of toluene were made at concentrations of 2500, 5000, 7500, and 10,000 PPM. To make a standard curve, 250 μl of vapor from one of the toluene standards was drawn into the gas-tight syringe, followed by 250 μl of vapor from the o-xylene internal standard ($n = 5$ per concentration). To measure toluene concentration in the vapor chamber, a 250-μl sample of vapor from the chamber was taken up into the gas-tight syringe followed by 250 μl o-xylene. The measured concentration of toluene obtained from the chamber after perfusion at the 4% vaporizer setting was 2946 ± 142 PPM, and at 8% it was 5860 ± 350 PPM. Because of the close agreement between the measured toluene concentration and the calculated value based on its vapor pressure, these values will herein be referred to as 2850 PPM and 5700 PPM, respectively.

Preparation of brain slices. Brain slices were prepared as previously described (Riegel and Williams, 2008; Beckley and Woodward, 2011). Briefly, rats were rapidly decapitated, brains were removed and placed in an ice-cold sucrose solution that contained (in mM): sucrose (200), KCl (1.9), NaH_2PO_4 (1.4), $CaCl_2$ (0.5), $MgCl_2$ (6), glucose (10), ascorbic acid (0.4), and $NaHCO_3$ (25); osmolarity 310–320 mOsm, bubbled with 95% O_2/5% CO_2 to maintain physiological pH. Sections containing the VTA were cut horizontally into 220- to 250-μm slices using a Leica VT1000 vibrating microtome with a double-walled chamber through which cooled (2–4°C) solution was circulated. Slices were collected and transferred to a warmed (32–34°C) chamber containing a carbogen-bubbled aCSF solution containing (in mM): NaCl (125), KCl (2.5), NaH_2PO_4 (1.4), $CaCl_2$ (2), $MgCl_2$ (1.3), glucose (10), ascorbic acid (0.4), and $NaHCO_3$ (25); osmolarity 310–320 mOsm. Slices were warmed for 30 min and then kept at room temperature for at least 45 min before beginning recordings.

Electrophysiology. Slices were transferred to a recording chamber and perfused with aCSF at 2 ml/min. Experiments were conducted at a bath

temperature of 32°C controlled by in-line and bath heaters (Warner Instruments). Neurons were visually identified under infrared light using an Olympus BX51WI microscope with Dodt gradient contrast imaging (Luigs and Neumann). Whole-cell patch-clamp recordings were performed on VTA neurons that contained red retrobeads (Lumafluor) as visualized by fluorescence microscopy. Recording pipettes with a resistance of 1–3 MΩ were filled with internal solution containing: (in mM): CsCl (120), HEPES (10), MgCl$_2$ (2), EGTA (1), Na$_2$ATP (2), NaGTP (0.3), 0.2% biocytin; osmolarity 295 mOsm, pH 7.3. In the AMPA rectification experiment, the internal solution also contained 100 μM spermine. Series resistance (R$_s$) was monitored throughout the recording, and an experiment was discontinued if R$_s$ exceeded 25 MΩ or changed >25%.

Currents were evoked using a tungsten concentric bipolar electrode. A 0.1-ms stimulus pulse was delivered at a setting that elicited a reliable, submaximal response from the recorded neuron. Data were acquired using an Axon MultiClamp 700B amplifier (Molecular Devices) and an ITC-18 digital interface (HEKA Instruments) controlled by AxographX software (Axograph Scientific). Recordings were filtered at 4 kHz, acquired at 10 kHz, and analyzed offline using AxographX software.

The recording aCSF was supplemented with 100 μM picrotoxin (Tocris Bioscience) to block GABA-A receptors and DL-APV (Abcam; 100 μM) was added when necessary to block NMDA receptors. Whole-cell mode was achieved while holding the cell at -70 mV. For AMPA/NMDA ratio measurements, neurons were held at -70 mV for 10 min and then the membrane potential was slowly changed to $+40$ mV. The setting for the stimulus pulse was then adjusted to yield an amplitude of $\sim$150 pA for the mixed glutamatergic excitatory postsynaptic current (EPSC), and this stimulus strength was used throughout the recording. Evoked excitatory currents were evoked every 30 s for 10 min, and then DL-APV was applied to isolate AMPA currents. The averaged AMPA current was subtracted from the averaged excitatory current to reveal the NMDA-mediated current, and peak amplitudes were measured to compute the AMPA/NMDA ratio. For AMPA rectification experiments, AMPA currents were evoked with a constant stimulus current at different holding potentials: $+40$, $+20$, 0, -30, and -70 mV. The AMPA rectification index was computed by dividing the slope of the regression line of AMPA peak current amplitudes at negative potentials by the slope of the regression line at positive holding potentials. Spontaneous EPSC events (at least 150 per cell) were detected and analyzed using the template-matching event-detection algorithm in AxographX. Detection parameters were set at amplitude >4 pA and acquired events were visually inspected before averaging.

Histology. Brain sections containing either the mPFC or NAcc were sliced into 300-μm slices, mounted onto gelatin-coated slides, and visualized with a Leica EZ4D stereomicroscope. For serial section analysis of retrobead injection and to verify cannula sites, brain sections were postfixed in 4% paraformaldehyde and then 30% sucrose. Slices (100 μm) containing the mPFC or NAc were prepared using a Thermo Scientific Microm HM550 cryostat. Slices were placed onto a gelatin-subbed slide, stained with cresyl violet, dehydrated, delipidated, and then coverslipped. For cannula verification, slices were imaged with the stereomicroscope. For serial section analysis of the retrobead injections, slices were imaged using the EVOS fl microscope (Advanced Microscopy Group).

DA neuron verification. Slices containing the VTA were fixed for 48 h in 4% paraformaldehyde, rinsed in 0.01 M PBS and then were incubated in 5% normal goat serum with 0.1% Triton-X for 7 min. Slices were incubated in rabbit anti-tyrosine hydroxylase (TH) and Avidin TexasRed for 24 h at 4°C. After PBS washes, slices were incubated in AlexaFluor488 goat anti-rabbit IgG for 2 h. Slices were mounted on glass slides and coverslipped using Prolong Antifade (Invitrogen) and then were imaged with a Zeiss LSM 510 confocal microscope.

Data analysis. For most experiments, a two-tailed independent *t* test or one-way ANOVA with Bonferroni *post hoc* testing was used to evaluate statistical significance. In cases when variance between groups was found to be significantly different, Kruskal–Wallis with Dunn's multiple-comparison *post hoc* test was used. A mixed ANOVA with *post hoc* Bonferroni testing was used to assess differences in sEPSC amplitude and
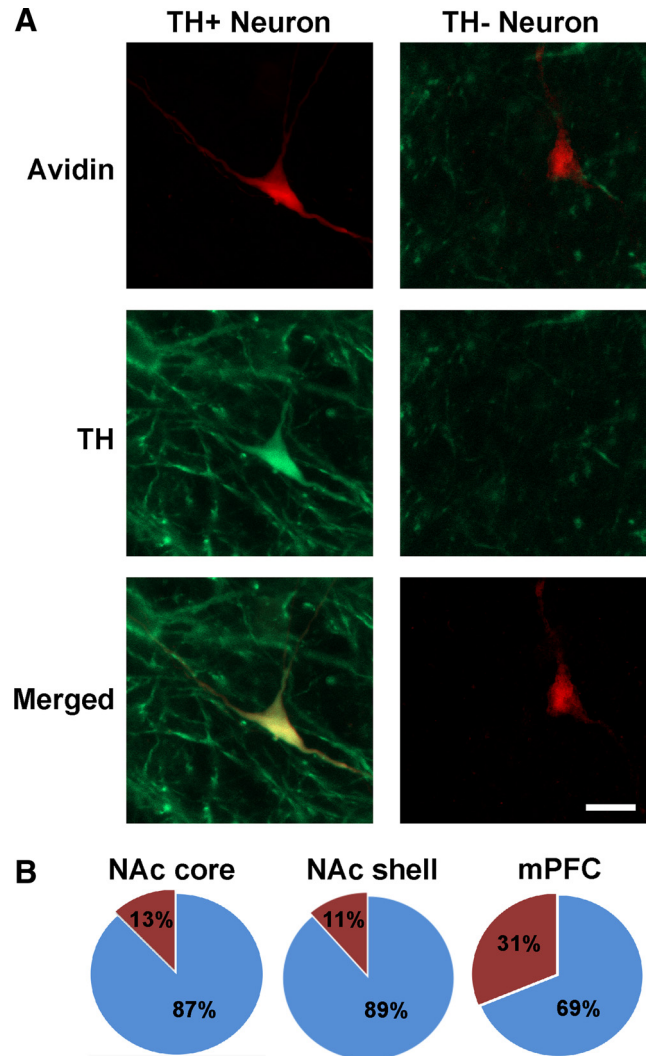
Figure 2. Immunohistochemistry for TH. ***A***, Examples of TH+ and TH− VTA neurons. Green indicates TH; and red, biocytin. Scale bar, 20 μm. ***B***, Proportion of TH+ recorded neurons per region that received the retrograde tracer microinjection; blue, TH+; red TH−. NAc core: 125 TH+; 18 TH−; NAc medial shell: 41 TH+; 5 TH−; mPFC: 11 TH+; 5 TH−.

interevent interval (IEI) cumulative probabilities, as well as current/voltage relationships of AMPA receptors in controls and toluene-treated subjects. In experiments where animals received an intra-PFC infusion before vapor exposure, a two-way ANOVA was used with a Bonferroni's *post hoc* test to test for significance. All tests of statistical significance were computed with GraphPad Prism software. In all experiments, the α value was set to 0.05. All values described in results are mean $\pm$ SEM.

Results

VTA TH+ neurons that project to the NAcc or mPFC

After patch-clamp recording, the DA phenotype of bead-labeled neurons was verified by the presence of TH immunoreactivity (Fig. 2A). Of the 143 VTA neurons labeled from NAcc-injected animals, 87% (125 cells) were TH+, whereas 13% (18) were TH−. Of the 46 VTA neurons labeled from NAcs-injected animals, 89% (41) were TH+, whereas 11% (5) were TH−. In mPFC-injected animals, a lower percentage (69%; 11 cells) of labeled neurons were TH+, whereas 31% (5) were TH−. The difference in proportion of TH+ to TH− neurons within each DA target region trended toward significance (Fig. 2B; $\chi^2(2) = 4.641$; $p = 0.098$) and is similar to that found in other studies (Lammel et al., 2011).

In vivo toluene exposure alters mesolimbic, but not mesocortical, DA neuron plasticity

Fluorescent retrobeads were injected into either NAcc or mPFC to allow for patch-clamp recordings from selective DA neuron subpopulations (Lammel et al., 2008). After allowing for retrograde transport for up to 3 weeks, subjects were exposed to either one of two concentrations of toluene or air as previously described. A brief exposure to 5700 PPM toluene, but not 2850 PPM toluene, significantly enhanced the AMPA/NMDA ratio in mesoaccumbens core DA neurons when measured 24 h after vapor exposure (Kruskal–Wallis: H(2) = 7.216; $p < 0.05$; Fig. 3C). AMPA-mediated EPSCs from 5700 PPM toluene exposed subjects were significantly larger than those from controls (air, mean ± SEM: 50.53 ± 5.80 pA, 5700 PPM toluene: 82.62 ± 9.13 pA, $t_{(13)} = 3.048$, $p < 0.01$), whereas NMDA-mediated currents showed a slight but nonsignificant reduction in amplitude (air: 69.03 ± 6.01 pA, toluene: 58.57 ± 4.95 pA, $t_{(13)} = 1.320$, not significant). There was also no difference in decay kinetics for NMDA EPSCs after toluene exposure (τ(slow), air: 257.60 ± 29.59 ms, toluene: 197.55 ± 19.98 ms, $t_{(13)} = 1.651$, not significant; τ(fast), air: 34.73 ± 4.60 ms, toluene: 69.82 ± 25.64 ms, Welch's corrected $t_{(6)} = 1.347$, not significant; data not shown). The increase in the AMPA/NMDA ratio after 5700 PPM toluene persisted for 3 d and returned to control values 7 d after exposure (Kruskal–Wallis: H(3) = 12.56, $p < 0.01$; Fig. 3D). However, there was no change in AMPA/NMDA ratio in air-only subjects measured 1, 3, or 7 d after the 1-h chamber exposure (data not shown), suggesting that baseline AMPA/NMDA ratios are stable over this narrow age range. In mesoaccumbens medial shell DA neurons, there was a significant enhancement in AMPA/NMDA ratio after toluene vapor when measured 24 h later, and this effect persisted for at least 21 d (one-way ANOVA: $F_{(4,40)} = 2.681$, $p < 0.05$; Fig. 3E). In contrast to mesolimbic DA neurons, high-dose toluene vapor had no effect on the AMPA/NMDA ratio in mesocortical DA neurons ($t_{(9)} = 0.12$, not significant; Fig. 4B).

Mechanism of toluene-induced alterations of mesolimbic DA neuron plasticity

The altered glutamatergic ratio in VTA DA neurons from toluene-exposed animals could have arisen from changes in either AMPA or NMDA-mediated transmission, although, as shown in the preceeding section, only the AMPA component was significantly altered in toluene-treated animals. However, it is important to note that measures of absolute amplitude may be biased because we constrained the size of the mixed glutamatergic EPSC to ~150 pA for each recording. Thus, even if AMPA currents were the only component that changed, this would likely involve a reduction in the apparent amplitude of NMDA EPSCs as well. To unambiguously examine whether toluene exposure enhances excitatory synaptic strength, we recorded AMPA-mediated sEPSCs from mesoaccumbens core neurons. A brief exposure to 5700 PPM toluene vapor increased the amplitude of sEPSCs compared with controls ($t_{(10)} = 2.58$, $p < 0.05$; Fig. 5B, inset), leading to a rightward shift in the cumulative probability of amplitude (mixed ANOVA: main effects of amplitude, $F_{(16,160)} = 308.4$, $p < 0.001$; and vapor treatment, $F_{(1,160)} = 5.90$, $p < 0.05$; and a significant amplitude × vapor treatment interaction, $F_{(16,160)} = 4.310$, $p < 0.001$; Fig. 5B). However, toluene vapor exposure had no effect on sEPSC frequency (IEI; $t_{(10)} = 0.098$, not significant; Fig. 5C, inset).

Other drugs of abuse, such as cocaine, have been shown to enhance the expression of GluA2 lacking receptors leading to increases in the degree of current rectification of AMPA-mediated EPSCs in VTA DA neurons (Argilli et al., 2008). To test whether toluene exposure produces similar effects, AMPA-mediated currents were evoked in mesoaccumbens core neurons at different holding potentials and a rectification index was calculated. One day after exposure to toluene vapor, AMPA currents were reduced at positive holding potentials (mixed ANOVA: main effect on voltage: $F_{(4,52)} = 1595$, $p < 0.001$; and a significant V × I interaction: $F_{(4,52)} = 6.692$, $p < 0.001$; Figure 6A), resulting in an increased rectification index of stimulus-evoked AMPA-mediated currents measured ($t_{(10)} = 2.891$, $p < 0.05$; Fig. 6C). These results suggest that toluene enhances the insertion of calcium-permeable GluA2-lacking AMPA receptors into postsynaptic DA neurons.

### PFC regulation of toluene-induced mesolimbic excitatory plasticity enhancement

Although commonly used drugs of abuse increase extracellular DA release in the NAc (Di Chiara and Imperato, 1988) and persistently enhance VTA DA excitatory synaptic transmission (Saal et al., 2003), acute exposure to toluene and other abused drugs, such as cocaine, also depress cortical activity (Trantham-Davidson and Lavin, 2004; Beckley and Woodward, 2011). Relevant to this study, findings from labeling studies reveal that mPFC terminals synapse on midbrain DA neurons that project back to the mPFC and onto GABA neurons that project to the NAcc (Carr and Sesack, 2000). VTA GABA interneurons also have extensive collateral connections to VTA DA neurons (Omelchenko and Sesack, 2009). This suggests that mPFC projections may provide a feedforward inhibition onto mesolimbic DA neurons, allowing the mPFC to gate the ability of natural and drug-induced rewards to induce plasticity in VTA mesolimbic neurons. To test this idea, rodents were infused in the prelimbic/infralimbic junction with a GABA receptor modulator 30 min before toluene vapor exposure. Picrotoxin and muscimol/baclofen were used in these studies as these compounds reliably excite (Hablitz, 1984) or inhibit (van Duuren et al., 2007) neuronal output, respectively, for prolonged periods. Alone, picrotoxin had no effect on AMPA/NMDA ratios of mesoaccumbens core DA neurons in air-exposed animals but completely blocked toluene's increase in this marker of plasticity (two-way ANOVA: main effects of pretreatment: $F_{(1,25)} = 5.51$; $p < 0.01$; and vapor treatment: $F_{(1,25)} = 11.19$, $p < 0.01$; and a significant pretreatment × vapor treatment interaction: $F_{(1,25)} = 4.776$, $p < 0.05$; Figure 7B). In contrast, in animals infused with muscimol/baclofen to reduce mPFC output, a concentration of toluene vapor (2850 PPM) that was previously ineffective (Fig. 3C) now robustly enhanced the AMPA/NMDA ratio of NAcc-projecting DA neurons. Importantly, muscimol/baclofen infusion had no effect in air-exposed animals (two-way ANOVA: main effects of pretreatment: $F_{(1,26)} = 5.641$, $p < 0.05$; and vapor treatment: $F_{(1,26)} = 4.556$, $p < 0.05$; Figure 7C), suggesting that altering mPFC output does not directly affect DA neuron plasticity in non–drug-exposed animals.

Discussion

A brief exposure to toluene persistently altered excitatory synaptic strength in mesolimbic, but not mesocortical, DA neurons. Although it cannot be ruled out that reductions in NMDA receptor signaling may underlie the increased AMPA/NMDA ratio in drug-exposed animals, the most parsimonious explanation is that calcium-permeable, GluA2-lacking AMPA receptors are upregulated after toluene exposure. Furthermore, the changes in mesolimbic synaptic glutamatergic activity were reversed or augmented by treatments designed to augment or inhibit mPFC out-
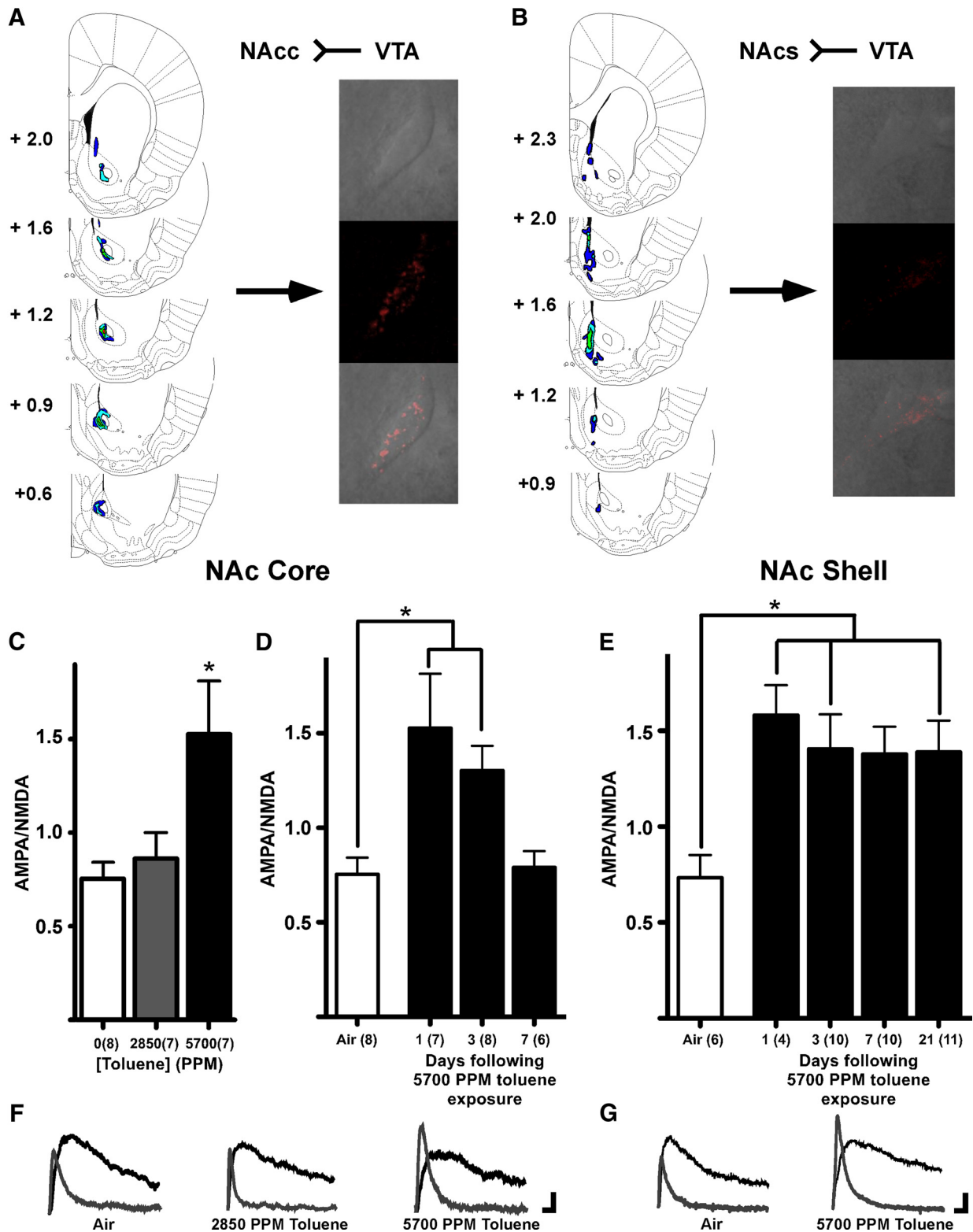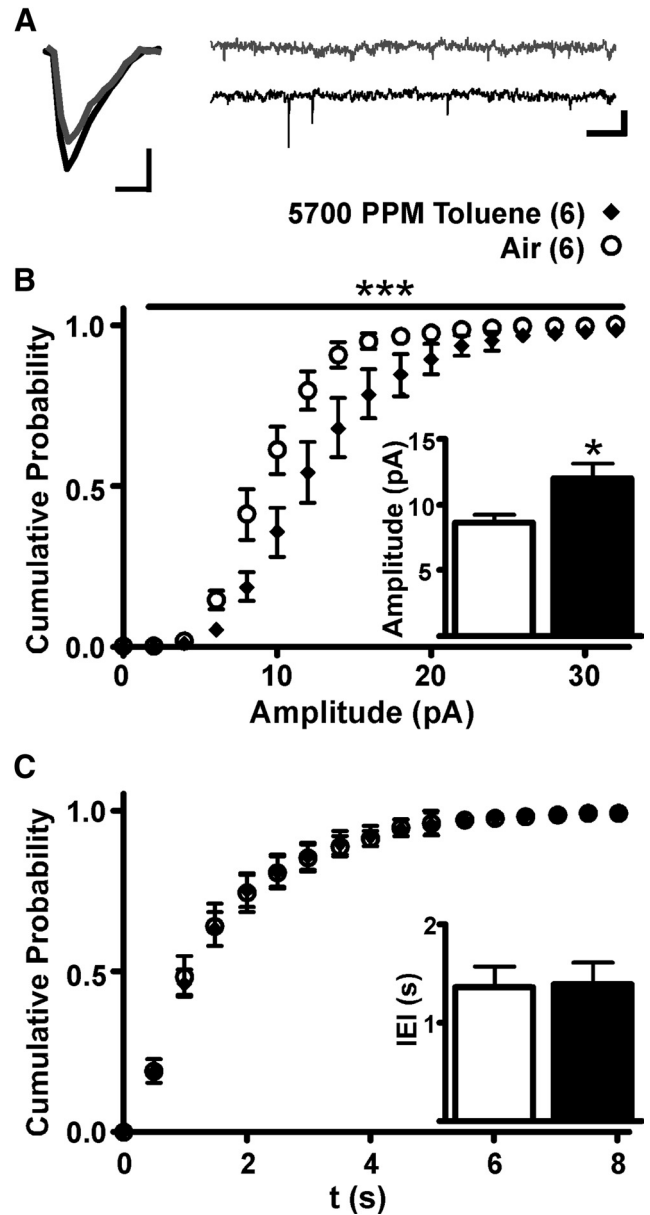
Figure 3. Toluene vapor enhances the AMPA/NMDA ratio in mesoaccumbens core and medial shell DA neurons. ***A***, Retrograde tracer injections into the NAcc result in retrobead expression in midbrain dopamine neurons. Left panels, Serial sections of both brain regions with a heat map of retrobead locations from 6 subjects. Values indicate distance from bregma (mm). Right panels, An example of retrobead expression (red) in a midbrain DA neuron. ***B***, Retrograde tracer injections into NAcs and retrobead expression in midbrain DA neuron. ***C***, AMPA/NMDA ratios 24 h after vapor chamber exposure in VTA DA neurons that project to the NAcc. *The 5700 PPM AMPA/NMDA ratio is higher than the ratio for the air control ($p < 0.05$, Kruskal–Wallis, Dunn's multiple-comparison test). ***D***, Time course of toluene effect on AMPA/NMDA ratio in mesoaccumbens core DA neurons. *AMPA/NMDA ratios 1 and 3 d after 5700 PPM toluene exposure are greater than air controls ($p < 0.05$, Kruskal–Wallis, Dunn's multiple-comparison test). ***E***, Time course of toluene effect on AMPA/NMDA ratio in mesoaccumbens medial shell neurons. *AMPA/NMDA ratios 1, 3, and 21 d after 5700 PPM toluene exposure are greater than air controls ($p < 0.05$, one-way ANOVA, Bonferroni's multiple-comparison test). ***F***, Example traces are AMPA-mediated (gray) and NMDA-mediated (black) currents in mesoaccumbens core neurons from subjects exposed to air, 2850 PPM toluene, or 5700 PPM toluene. Calibration: 20 pA, 10 ms. ***G***, Example traces from subjects exposed to air or 5700 PPM toluene. Calibration: 20 pA, 10 ms.
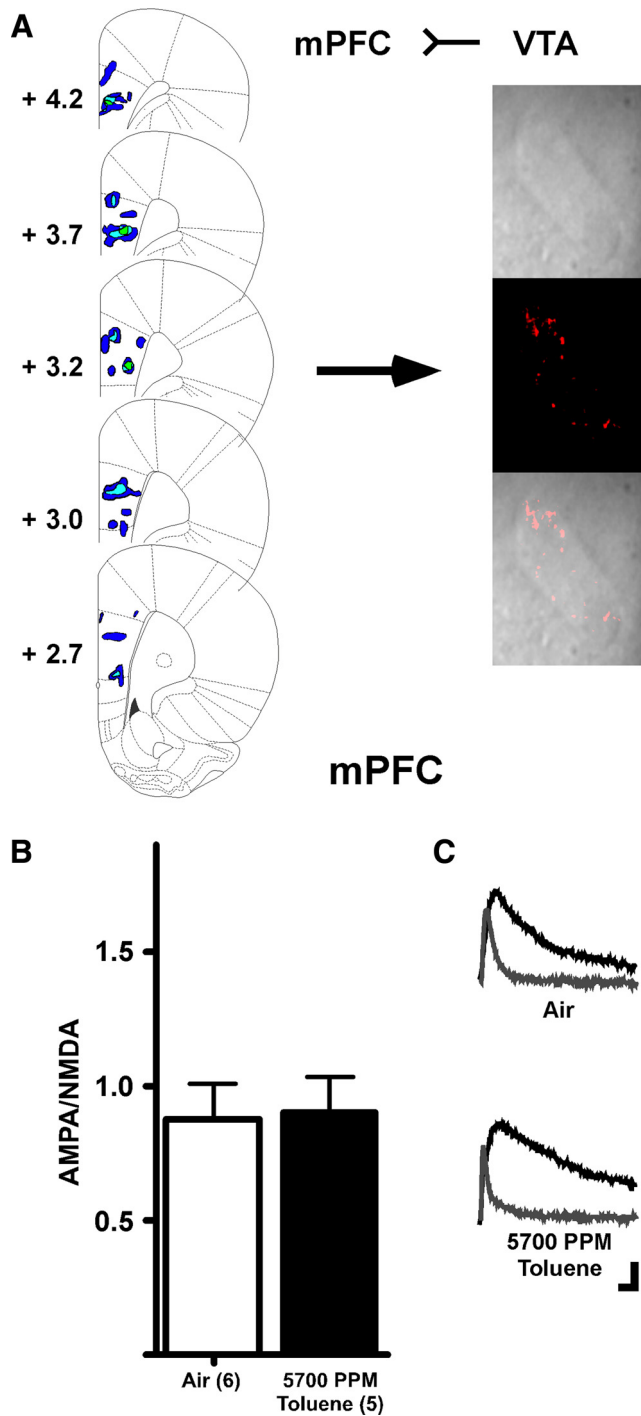
Figure 4. Toluene vapor has no effect on mesocortical DA neurons. **A**, Retrograde tracer injections into mPFC and retrobead expression in a midbrain DA neuron. **B**, Summary of effects of toluene on AMPA/NMDA ratio in mesocortical DA neurons. **C**, Example traces from subjects exposed to air or 5700 PPM toluene. Calibration: 20 pA, 10 ms.

Figure 5. *In vivo* toluene exposure increases sEPSC amplitude, but not frequency, in mesoaccumbens core DA neurons. **A**, Averaged sEPSC traces from air-exposed (gray) and toluene-exposed subjects (black) (calibration: 5 ms, 5 pA) and an extended EPSC recording (calibration: 0.5 s, 25 pA, 0.5 s). **B**, Cumulative probability chart of sEPSC amplitude from animals exposed to 5700 PPM toluene or air. ***Significant amplitude × vapor treatment interaction ($p < 0.001$, mixed ANOVA). Inset: Average sEPSC amplitude for subjects exposed to air or toluene. *$p < 0.05$ (t test). **C**, Cumulative probability chart of sEPSC IEI for toluene vapor and air controls. Inset, Average sEPSC IEI for toluene and air control.

put, respectively. These findings confirm that toluene, like other abused drugs, impacts portions of the neurocircuitry associated with the development and maintenance of addiction and implicates the mPFC as an important mediator of this action.

Toluene has a psychopharmacological profile similar to that of CNS depressants, such as ethanol (Bowen et al., 2006). After acute exposure to toluene, a biphasic pattern of activity occurs with behavioral excitation followed by depressant-like effects, such as sedation and ataxia (Kurtzman et al., 2001). Toluene also

shares discriminative stimulus properties with ethanol, suggesting overlapping sites of action between these compounds (Rees et al., 1987; Evans and Balster, 1991; Bowen, 2009). Furthermore, toluene acts similarly to other abused drugs in terms of its impact on the mesolimbic dopamine system and related behavioral models of addiction. Thus, rats express conditioned place preference for a toluene-paired environment (Lee et al., 2006), and mice will self-administer toluene intravenously (Blokhina et al., 2004). Exposure to 7000 PPM toluene vapor increases extracellular DA levels in the NAc and PFC (Koga et al., 2007), consistent with its ability to increase the firing of VTA DA neurons (Riegel et al., 2007). Although solvents are often overlooked as drugs of
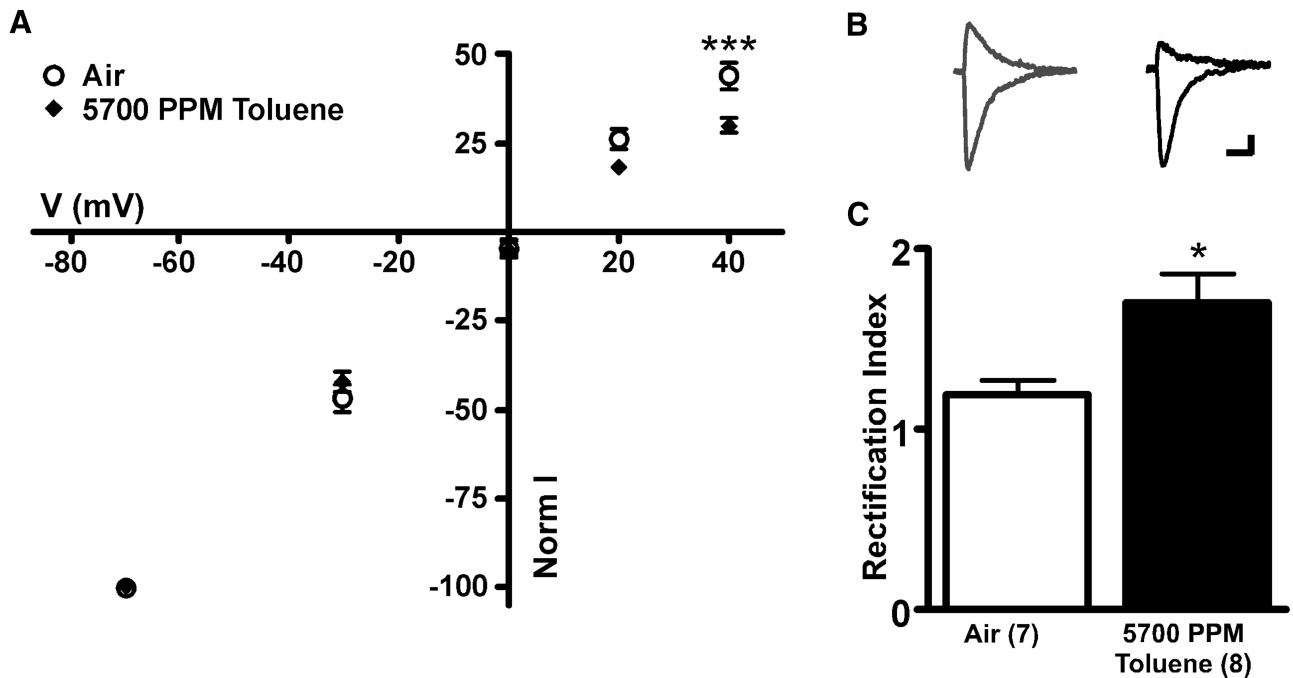
Figure 6. *In vivo* toluene exposure alters AMPA receptor rectification in mesoaccumbens core DA neurons. *A*, I–V relationship for evoked EPSC normalized peak amplitudes at varying holding potentials in subjects exposed to toluene vapor and air. ***Current output at +40 mV holding potential is different between groups ($p < 0.001$, mixed ANOVA, Bonferroni multiple-comparison test). *B*, Sample AMPA traces at +40 mV and −70 mV holding potentials for air controls (gray) and toluene-exposed subjects (black). Calibration: 5 ms, 25 pA. *C*, Summary of toluene effect on rectification index. *AMPA rectification index for toluene-treated subjects is different from air control ($p < 0.05$, t test).
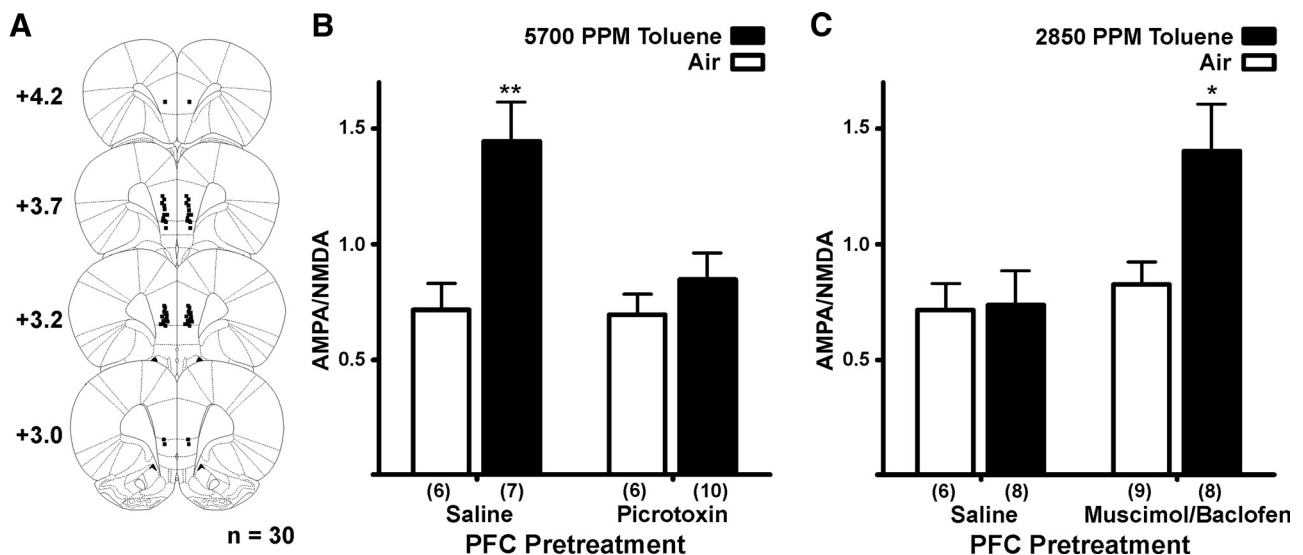
Figure 7. PFC output regulates toluene's effect on AMPA/NMDA ratio in mesoaccumbens core DA neurons. *A*, Microinjection cannula placements in the medial prefrontal cortex. Values are distance from bregma (mm). *B*, Summary of effects of an intra-mPFC picrotoxin infusion (100 ng) before vapor chamber exposure. **Saline mPFC infusion/5700 PPM toluene group is different from all other groups ($p < 0.01$ for each comparison, two-way ANOVA, Bonferroni *post hoc* test). *C*, Summary of effects of an intra-mPFC muscimol/baclofen infusion (3.5 mg/130 ng) before vapor chamber exposure. *Muscimol/baclofen mPFC infusion/2850 PPM toluene group is different from all other groups ($p < 0.05$ for each comparison, two-way ANOVA, Bonferroni *post hoc* test).

abuse, the most recent Monitoring the Future annual study (Johnston et al., 2012) shows that the prevalence of inhalant use among adolescents is similar to or greater than that of other abused drugs. Given the potential for adverse effects of solvent use in younger individuals, studies examining the molecular and cellular mechanisms of toluene action are critical for understanding the impact these agents have on brain function and behavior.

In this study, a brief *in vivo* exposure to toluene vapor significantly enhanced excitatory synaptic strength in mesoaccumbens core and medial shell DA neurons. Intriguingly, although gluta-

matergic synaptic transmission was altered for at least 21 d in mesoaccumbens medial shell neurons, similar to that of cocaine (Lammel et al., 2011), increases in synaptic strength in mesoaccumbens core neurons was more limited (<7 d), suggesting differences in the sensitivity of DA neuron subpopulations to toluene. These findings are consistent with those from previous studies showing that, although cocaine increases extracellular DA in both core and shell regions of the ventral striatum (Ito et al., 2000; Owesson-White et al., 2009), there is a larger increase in the medial shell compared with the core (Aragona et al., 2008). The

mechanism underlying the differential sensitivity of mesolimbic DA neurons to drugs of abuse is unknown but may be related to the different neural circuits that mid-brain DA neurons interact with to regulate motivated behaviors and well-learned motor action plans. For example, efferent's from medium spiny neurons in NAc core target basal ganglia nuclei, such as ventral pallidum and substantia nigra pars reticulata (Maurice et al., 1999), and the core projection to ventral pallidum is into the dorsolateral division (Maurice et al., 1997) that only has outputs to basal ganglia nuclei (Ikemoto, 2007; Humphries and Prescott, 2010). In contrast, medial shell medium spiny neurons project to the medial ventral pallidum (Ikemoto, 2007), which then projects to nuclei outside the basal ganglia, such as lateral hypothalamus, pedunculopontine nucleus, and mediodorsal thalamus (Groenewegen et al., 1993). Medial shell neurons also have direct outputs to regions outside of the basal ganglia circuitry (Usuda et al., 1998). These findings indicate that the NAcs and NAcc are critical components of distinct yet overlapping cortico-striato-pallidothalamic circuits. Furthermore, midbrain dopamine nuclei are connected to the striatum via a hierarchical, ascending spiral circuit, with the NAcc being downstream from, and influenced by, the NAcs, and the dorsal striatal neurons being downstream from both (Haber et al., 2000; Everitt and Robbins, 2005).

After a single use of a drug, such as cocaine, synaptic transmission in nigrostriatal DA neurons is unaffected (Lammel et al., 2011). However, with repeated drug use, alterations in the dorsomedial striatum and dorsolateral striatum are hypothesized to contribute to the development of addiction pathology (Everitt and Robbins, 2005; Hyman et al., 2006). Whereas the dorsomedial striatum largely encodes action-outcome associations that are essential for goal directed behaviors, dorsolateral striatum neurons drive habit formation (O'Doherty et al., 2004; Balleine et al., 2007; Tanaka et al., 2008). As such, current thinking suggests that acute drug exposure first induces adaptations in the ventral striatal network that then spread to the dorsomedial striatum and dorsolateral striatum as drug use becomes more chronic. These network adaptations may reflect the transition from reward-based behavior generated by a drug's valence and salience, to chronic drug taking that exhibits characteristics of an habitual motor-driven response (Everitt and Robbins, 2005; Koob and Volkow, 2010). The data from the present study reinforce this idea by showing that a brief exposure to another important class of drugs, abused inhalants, elicits robust and selective changes in glutamatergic signaling of mesoaccumbens dopamine neurons.

An intriguing finding of the present study is the critical role that the mPFC plays in regulating toluene's effects on mesolimbic DA neuron synaptic properties. In previous studies, mPFC stimulation has been shown to induce either excitation or inhibition of DA neuron activity (Tong et al., 1996; Aston-Jones et al., 2009; Lodge, 2011), possibly depending on the DA subpopulation that is being recorded. mPFC terminals synapse onto dopaminergic neurons that project back to the mPFC, whereas mPFC inputs also form synapses on GABAergic neurons that project to the NAc (Carr and Sesack, 2000). GABAergic interneurons within the VTA also synapse onto mesolimbic DA neurons (Omelchenko and Sesack, 2009). Whereas a comprehensive tract-tracing study reported that the VTA receives input from the mPFC (Gabbott et al., 2005), a recent report using a modified rabies virus to identify synaptic inputs reveals that VTA DA neurons receive very few inputs from either infralimbic or prelimbic cortices (Watabe-Uchida et al., 2012). Functionally, activation of VTA GABA interneurons interrupts reward consumption (van Zessen et al., 2012) and can produce conditioned place aversion

(Tan et al., 2012). Whereas Tong et al. (1996) showed that mPFC drives burst-like activity in DA neurons, a 1.0-mA stimulation of mPFC produced pure excitation in only 30% of DA neurons, with 52% percent showing a brief excitation followed by a prolonged inhibition, and 15% showing just inhibition. These experiments illustrate that, although DA neuronal response to mPFC stimulation is complex, inhibition of DA neurons predominates. Similarly, dopamine neurons display a slow oscillation in membrane potential that is coherent with, but in reverse phase to, that of mPFC neurons, suggesting an inhibitory intermediate cell type (Gao et al., 2007). In addition, the mPFC also projects to the GABAergic tail of the VTA (tVTA) (Jhou et al., 2009; Kaufling et al., 2009) that sends inhibitory projections to the VTA resulting in inhibition of DA neuron activity (Kaufling et al., 2009). The tVTA also receives heavy excitatory input from the lateral habenula (Jhou et al., 2009), that itself is innervated by the mPFC (Kim and Lee, 2012). Increased lateral habenula output thus excites tVTA neurons resulting in dopamine neuron inhibition (Christoph et al., 1986; Ji and Shepard, 2007) and disruptions in reward-based responding (Lammel et al., 2012; Stamatakis and Stuber, 2012). Therefore, based on results presented here and from previously published circuitry studies, we speculate that mPFC output inhibits mesolimbic dopamine neuron activity through several routes, including direct excitation of intra-VTA GABAergic interneurons and tVTA GABA projection neurons, and enhancement of lateral habenula activity that also drives tVTA-mediated inhibition of VTA DA neurons. Further studies, using techniques such as optogenetics (Zhang et al., 2007), will be needed to determine which of these mPFC circuits are involved in regulating toluene's action on plasticity of mesolimbic DA neurons.

We showed in a prior study that toluene induces a long-lasting endocannabinoid-dependent suppression of glutamatergic signaling from deep-layer mPFC pyramidal neurons (Beckley and Woodward, 2011). Together with the findings of the present study, these results suggest that a brief exposure to intoxicating concentrations of toluene vapor alters the mesolimbic dopamine system in two distinct ways: one via direct excitatory actions on intrinsic mechanisms that regulate mesolimbic DA neuron firing activity (Riegel et al., 2007) and the other by depressing top-down cortical activity, thus disinhibiting mesolimbic DA neuron plasticity. Because pharmacologically diverse drugs of abuse share the ability to alter VTA DA excitability, these findings also suggest that changes in mPFC output either during acute drug intoxication or as a result of long-term drug use may be a critical element in the continued use of abused drugs. This study is a first step in showing a more critical role of mPFC in the initial alterations that occur in the mesolimbic dopamine system after an acute exposure to a drug of abuse.

References

Aragona BJ, Cleaveland NA, Stuber GD, Day JJ, Carelli RM, Wightman RM (2008) Preferential enhancement of dopamine transmission within the nucleus accumbens shell by cocaine is attributable to a direct increase in phasic dopamine release events. J Neurosci 28:8821–8831. CrossRef Medline

Argilli E, Sibley DR, Malenka RC, England PM, Bonci A (2008) Mechanism and time course of cocaine-induced long-term potentiation in the ventral tegmental area. J Neurosci 28:9092–9100. CrossRef Medline

Aston-Jones G, Smith RJ, Moorman DE, Richardson KA (2009) Role of lateral hypothalamic orexin neurons in reward processing and addiction. Neuropharmacology 56 [Suppl 1]:112–121. CrossRef Medline

Balleine BW, Delgado MR, Hikosaka O (2007) The role of the dorsal striatum in reward and decision-making. J Neurosci 27:8161–8165. CrossRef Medline

Beckley JT, Woodward JJ (2011) The abused inhalant toluene differentially modulates excitatory and inhibitory synaptic transmission in deep-layer neurons of the medial prefrontal cortex. Neuropsychopharmacology 36:1531–1542. CrossRef Medline

Björklund A, Dunnett SB (2007) Dopamine neuron systems in the brain: an update. Trends Neurosci 30:194–202. CrossRef Medline

Blokhina EA, Dravolina OA, Bespalov AY, Balster RL, Zvartau EE (2004) Intravenous self-administration of abused solvents and anesthetics in mice. Eur J Pharmacol 485:211–218. CrossRef Medline

Bowen SE (2009) Time course of the ethanol-like discriminative stimulus effects of abused inhalants in mice. Pharmacol Biochem Behav 91:345–350. CrossRef Medline

Bowen SE, Batis JC, Paez-Martinez N, Cruz SL (2006) The last decade of solvent research in animal models of abuse: mechanistic and behavioral studies. Neurotoxicol Teratol 28:636–647. CrossRef Medline

Carr DB, Sesack SR (2000) Projections from the rat prefrontal cortex to the ventral tegmental area: target specificity in the synaptic associations with mesoaccumbens and mesocortical neurons. J Neurosci 20:3864–3873. Medline

Christoph GR, Leonzio RJ, Wilcox KS (1986) Stimulation of the lateral habenula inhibits dopamine-containing neurons in the substantia nigra and ventral tegmental area of the rat. J Neurosci 6:613–619. Medline

Di Chiara G, Imperato A (1988) Drugs abused by humans preferentially increase synaptic dopamine concentrations in the mesolimbic system of freely moving rats. Proc Natl Acad Sci U S A 85:5274–5278. CrossRef Medline

Evans EB, Balster RL (1991) CNS depressant effects of volatile organic solvents. Neurosci Biobehav Rev 15:233–241. CrossRef Medline

Everitt BJ, Robbins TW (2005) Neural systems of reinforcement for drug addiction: from actions to habits to compulsion. Nat Neurosci 8:1481–1489. CrossRef Medline

Ford CP, Mark GP, Williams JT (2006) Properties and opioid inhibition of mesolimbic dopamine neurons vary according to target location. J Neurosci 26:2788–2797. CrossRef Medline

Gabbott PL, Warner TA, Jays PR, Salway P, Busby SJ (2005) Prefrontal cortex in the rat: projections to subcortical autonomic, motor, and limbic centers. J Comp Neurol 492:145–177. CrossRef Medline

Gao M, Liu CL, Yang S, Jin GZ, Bunney BS, Shi WX (2007) Functional coupling between the prefrontal cortex and dopamine neurons in the ventral tegmental area. J Neurosci 27:5414–5421. CrossRef Medline

Gerasimov MR, Schiffer WK, Marstellar D, Ferrieri R, Alexoff D, Dewey SL (2002) Toluene inhalation produces regionally specific changes in extracellular dopamine. Drug Alcohol Depend 65:243–251. CrossRef Medline

Groenewegen HJ, Berendse HW, Haber SN (1993) Organization of the output of the ventral striatopallidal system in the rat: ventral pallidal efferents. Neuroscience 57:113–142. CrossRef Medline

Haber SN, Fudge JL, McFarland NR (2000) Striatonigrostriatal pathways in primates form an ascending spiral from the shell to the dorsolateral striatum. J Neurosci 20:2369–2382. Medline

Hablitz JJ (1984) Picrotoxin-induced epileptiform activity in hippocampus: role of endogenous versus synaptic factors. J Neurophysiol 51:1011–1027. Medline

Heikkinen AE, Möykkynen TP, Korpi ER (2009) Long-lasting modulation of glutamatergic transmission in VTA dopamine neurons after a single dose of benzodiazepine agonists. Neuropsychopharmacology 34:290–298. CrossRef Medline

Humphries MD, Prescott TJ (2010) The ventral basal ganglia, a selection mechanism at the crossroads of space, strategy, and reward. Prog Neurobiol 90:385–417. CrossRef Medline

Hyman SE, Malenka RC, Nestler EJ (2006) Neural mechanisms of addiction: the role of reward-related learning and memory. Annu Rev Neurosci 29:565–598. CrossRef Medline

Ikemoto S (2007) Dopamine reward circuitry: two projection systems from the ventral midbrain to the nucleus accumbens-olfactory tubercle complex. Brain Res Rev 56:27–78. CrossRef Medline

Ito R, Dalley JW, Howes SR, Robbins TW, Everitt BJ (2000) Dissociation in conditioned dopamine release in the nucleus accumbens core and shell in response to cocaine cues and during cocaine-seeking behavior in rats. J Neurosci 20:7489–7495. Medline

Jhou TC, Geisler S, Marinelli M, Degarmo BA, Zahm DS (2009) The mesopontine rostromedial tegmental nucleus: a structure targeted by the lateral habenula that projects to the ventral tegmental area of Tsai and substantia nigra compacta. J Comp Neurol 513:566–596. CrossRef Medline

Ji H, Shepard PD (2007) Lateral habenula stimulation inhibits rat midbrain dopamine neurons through a GABA(A) receptor-mediated mechanism. J Neurosci 27:6923–6930. CrossRef Medline

Johnston LD, O'Malley PM, Bachman JG, Schulenberg JE (2012) Monitoring the Future national survey results on drug use, 1975–2011. Volume I: Secondary school students. Bethesda, MD: National Institute on Drug Abuse.

Kaufling J, Veinante P, Pawlowski SA, Freund-Mercier MJ, Barrot M (2009) Afferents to the GABAergic tail of the ventral tegmental area in the rat. J Comp Neurol 513:597–621. CrossRef Medline

Kim U, Lee T (2012) Topography of descending projections from anterior insular and medial prefrontal regions to the lateral habenula of the epithalamus in the rat. Eur J Neurosci 35:1253–1269. CrossRef Medline

Koga Y, Higashi S, Kawahara H, Ohsumi T (2007) Toluene inhalation increases extracellular noradrenaline and dopamine in the medial prefrontal cortex and nucleus accumbens in freely-moving rats. J Kyushu Dent Soc 61:39–54. CrossRef

Koob GF, Volkow ND (2010) Neurocircuitry of addiction. Neuropsychopharmacology 35:217–238. CrossRef Medline

Kurtzman TL, Otsuka KN, Wahl RA (2001) Inhalant abuse by adolescents. J Adolesc Health 28:170–180. CrossRef Medline

Lammel S, Hetzel A, Häckel O, Jones I, Liss B, Roeper J (2008) Unique properties of mesoprefrontal neurons within a dual mesocorticolimbic dopamine system. Neuron 57:760–773. CrossRef Medline

Lammel S, Ion DI, Roeper J, Malenka RC (2011) Projection-specific modulation of dopamine neuron synapses by aversive and rewarding stimuli. Neuron 70:855–862. CrossRef Medline

Lammel S, Lim BK, Ran C, Huang KW, Betley MJ, Tye KM, Deisseroth K, Malenka RC (2012) Input-specific control of reward and aversion in the ventral tegmental area. Nature 491:212–217. CrossRef Medline

Lee DE, Gerasimov MR, Schiffer WK, Gifford AN (2006) Concentration-dependent conditioned place preference to inhaled toluene vapors in rats. Drug Alcohol Depend 85:87–90. CrossRef Medline

Lodge DJ (2011) The medial prefrontal and orbitofrontal cortices differentially regulate dopamine system function. Neuropsychopharmacology 36:1227–1236. CrossRef Medline

Lubman DI, Yucel M, Lawrence AJ (2008) Inhalant abuse among adolescents: neurobiological considerations. Br J Pharmacol 154:316–326. CrossRef Medline

Lüscher C, Malenka RC (2011) Drug-evoked synaptic plasticity in addiction: from molecular changes to circuit remodeling. Neuron 69:650–663. CrossRef Medline

Mameli M, Halbout B, Creton C, Engblom D, Parkitna JR, Spanagel R, Lüscher C (2009) Cocaine-evoked synaptic plasticity: persistence in the VTA triggers adaptations in the NAc. Nat Neurosci 12:1036–1041. CrossRef Medline

Mansvelder HD, McGehee DS (2000) Long-term potentiation of excitatory inputs to brain reward areas by nicotine. Neuron 27:349–357. CrossRef Medline

Maurice N, Deniau JM, Menetrey A, Glowinski J, Thierry AM (1997) Position of the ventral pallidum in the rat prefrontal cortex-basal ganglia circuit. Neuroscience 80:523–534. CrossRef Medline

Maurice N, Deniau JM, Glowinski J, Thierry AM (1999) Relationships between the prefrontal cortex and the basal ganglia in the rat: physiology of the cortico-nigral circuits. J Neurosci 19:4674–4681. Medline

O'Doherty J, Dayan P, Schultz J, Deichmann R, Friston K, Dolan RJ (2004) Dissociable roles of ventral and dorsal striatum in instrumental conditioning. Science 304:452–454. CrossRef Medline

Omelchenko N, Sesack SR (2009) Ultrastructural analysis of local collaterals of rat ventral tegmental area neurons: GABA phenotype and synapses onto dopamine and GABA cells. Synapse 63:895–906. CrossRef Medline

Owesson-White CA, Ariansen J, Stuber GD, Cleaveland NA, Cheer JF, Wightman RM, Carelli RM (2009) Neural encoding of cocaine-seeking behavior is coincident with phasic dopamine release in the accumbens core and shell. Eur J Neurosci 30:1117–1127. CrossRef Medline

Paxinos G, Watson C (2005) The rat brain in stereotaxic coordinates, Ed 5. Burlington, MA: Elsevier Academic.

Rees DC, Knisely JS, Breen TJ, Balster RL (1987) Toluene, halothane, 1,1,1-trichloroethane and oxazepam produce ethanol-like discriminative stimulus effects in mice. J Pharmacol Exp Ther 243:931–937. Medline

Riegel AC, Williams JT (2008) CRF facilitates calcium release from intracellular stores in midbrain dopamine neurons. Neuron 57:559–570. CrossRef Medline

Riegel AC, Zapata A, Shippenberg TS, French ED (2007) The abused inhalant toluene increases dopamine release in the nucleus accumbens by directly stimulating ventral tegmental area neurons. Neuropsychopharmacology 32:1558–1569. CrossRef Medline

Saal D, Dong Y, Bonci A, Malenka RC (2003) Drugs of abuse and stress trigger a common synaptic adaptation in dopamine neurons. Neuron 37:577–582. CrossRef Medline

Stamatakis AM, Stuber GD (2012) Activation of lateral habenula inputs to the ventral midbrain promotes behavioral avoidance. Nat Neurosci 15: 1105–1107. CrossRef Medline

Tanaka SC, Balleine BW, O'Doherty JP (2008) Calculating consequences: brain systems that encode the causal effects of actions. J Neurosci 28: 6750–6755. CrossRef Medline

Tan KR, Yvon C, Turiault M, Mirzabekov JJ, Doehner J, Labouèbe G, Deisseroth K, Tye KM, Lüscher C (2012) GABA neurons of the VTA drive conditioned place aversion. Neuron 73:1173–1183. CrossRef Medline

Tong ZY, Overton PG, Clark D (1996) Stimulation of the prefrontal cortex in the rat induces patterns of activity in midbrain dopaminergic neurons which resemble natural burst events. Synapse 22:195–208. CrossRef Medline

Trantham-Davidson H, Lavin A (2004) Acute cocaine administration depresses cortical activity. Neuropsychopharmacology 29:2046–2051. CrossRef Medline

Ungless MA, Whistler JL, Malenka RC, Bonci A (2001) Single cocaine exposure in vivo induces long-term potentiation in dopamine neurons. Nature 411:583–587. CrossRef Medline

Usuda I, Tanaka K, Chiba T (1998) Efferent projections of the nucleus accumbens in the rat with special reference to subdivision of the nucleus: biotinylated dextran amine study. Brain Res 797:73–93. CrossRef Medline

van Duuren E, van der Plasse G, van der Blom R, Joosten RN, Mulder AB, Pennartz CM, Feenstra MG (2007) Pharmacological manipulation of neuronal ensemble activity by reverse microdialysis in freely moving rats: a comparative study of the effects of tetrodotoxin, lidocaine, and muscimol. J Pharmacol Exp Ther 323:61–69. CrossRef Medline

van Zessen R, Phillips JL, Budygin EA, Stuber GD (2012) Activation of VTA GABA neurons disrupts reward consumption. Neuron 73:1184–1194. CrossRef Medline

Watabe-Uchida M, Zhu L, Ogawa SK, Vamanrao A, Uchida N (2012) Whole-brain mapping of direct inputs to midbrain dopamine neurons. Neuron 74:858–873. CrossRef Medline

Zhang F, Aravanis AM, Adamantidis A, de Lecea L, Deisseroth K (2007) Circuit-breakers: optical technologies for probing neural signals and systems. Nat Rev Neurosci 8:577–581. CrossRef Medline